Synthesis of the Anion $[Ru_3H(\mu_3\text{-}PPh)(CO)_9]^-$ and its Reactions with Complexes of Re, Rh, Ir, Cu, Ag, and Au to give Heterometallic Clusters containing a Triruthenium Unit: Crystal Structures of the Complexes $[Ru_3Rh_2(\mu_4\text{-}PPh)(CO)_{13}(PEt_3)]$ and $[Ru_3\{\mu\text{-}Au(PMe_2Ph)\}(\mu\text{-}H)(\mu_3\text{-}PPh)(CO)_9]$ †

Martin J. Mays,* Paul R. Raithby, and Philip L. Taylor
University Chemical Laboratory, Lensfield Road, Cambridge CB2 1EW
Kim Henrick
School of Chemistry, The Polytechnic of North London, Holloway Road, London N7 8DB

Deprotonation of $[Ru_3H_2(\mu_3\text{-}PPh)(CO)_9]$ with base gives the anion $[Ru_3H(\mu_3\text{-}PPh)(CO)_9]^-$ which has been isolated as its $[N(PPh_3)_2]^+$ salt. This anion reacts with cationic complexes of Re, Rh, Ir, and Au, and with $[\{CuI(PEt_3)\}_4]$ and $[\{AgI(PEt_3)\}_4]$, to give heterometallic complexes containing a triruthenium unit. With Re, Rh, Ir, Cu, Ag, and Au, tetranuclear complexes are obtained and structures in which the heterometal atom (M') either bridges one edge of [M' = Cu, Ag, or Au] or caps the Ru_3 triangle [M' = Re, Rh, or Ir] are proposed. In the case of the gold complex, $[Ru_3\{\mu\text{-}Au(PMe_2Ph)\}(\mu\text{-}H)(\mu_3\text{-}PPh)(CO)_9]$, this proposal has been confirmed by an *X*-ray analysis. This complex crystallises in space group $P2_1/c$ with $a = 8.805(3)$, $b = 20.195(7)$, $c = 16.683(6)$ Å, $\beta = 100.62(2)°$, and $Z = 4$. The structure was solved by a combination of direct methods and Fourier-difference techniques, and refined by blocked-cascade least squares to $R = 0.067$ for 1 398 unique diffractometer data with $F > 5\sigma(F)$. The reaction of the triruthenium anion with $[Rh(CO)_3(PR_3)_2]^+$ (R = Et or Ph) gives, in addition to the tetranuclear complexes, the pentanuclear complexes $[Ru_3Rh_2(PPh)(CO)_{13}(PR_3)]$. An *X*-ray analysis of the complex with R = Et reveals a square-pyramidal array of metal atoms with a μ_4-PPh ligand capping two of the Ru and the two Rh atoms to give an overall distorted octahedral geometry. This complex crystallises in space group $C2/c$ with $a = 20.257(5)$, $b = 9.679(3)$, $c = 34.726(5)$ Å, $\beta = 90.24(2)°$, and $Z = 8$. The structure was solved using the same techniques as for the Ru_3Au complex and refined to $R = 0.034$ for 4 708 diffractometer data with $F > 6\sigma(F)$.

We have recently reported [1] the synthesis and *X*-ray characterisation of the μ_3-phosphido-complex $[Ru_3(\mu\text{-}H)_2(\mu_3\text{-}PPh)(CO)_9]$ (1), and this complex has also been prepared in several other laboratories.[2-4] The interest in complexes of this type stems from the hope that the capping ligand may inhibit their fragmentation into mononuclear species during studies of their reactivity and catalytic properties. These hopes have been partially realised [5,6] although bridging and capping phosphorus groups may sometimes participate in the reactions of complexes in which they are present.[7,8]

A triruthenium complex of particular interest is the anion $[Ru_3H(CO)_{11}]^-$, since this anion has been implicated as a catalytically active species, *e.g.* in the water-gas shift reaction [9,10] and in the synthesis of ethylene glycol from CO and H_2.[11] In this paper we report the synthesis of the anion $[Ru_3H(\mu_3\text{-}PPh)(CO)_9]^-$ which may be regarded as a phosphorus-capped analogue of $[Ru_3H(CO)_{11}]^-$, with the μ_3-PPh group acting as a four-electron donor in place of two CO groups. We report also the reactions of this anion with (mainly cationic) complexes of other metals to give mixed-metal clusters, two of which have been characterised by *X*-ray analyses. A preliminary account of part of this work has been published.[12]

† 1,2-μ-Carbonyl-1,2,2,3,3,3,4,4,4,5,5,5-dodecacarbonyl-1,2,3,4-μ_4-phenylphosphido-1-triethylphosphinedirhodiumtriruthenium(*Rh–Rh*)(4 *Rh–Ru*)(3 *Ru–Ru*) and 1,1,1,2,2,2,3,3,3-nonacarbonyl-1,2-μ-dimethylphenylphosphineaurio-1,3-μ-hydrido-μ_3-phenylphosphido-triruthenium(3 *Ru–Ru*).

Supplementary data available (No. SUP 23863, 46 pp.): H-atom co-ordinates, thermal parameters, observed and calculated structure factors. See Instructions for Authors, *J. Chem. Soc., Dalton Trans.*, 1984, Issue 1, pp. xvii—xix.

Results and Discussion

(*a*) *Preparation and properties of* $[N(PPh_3)_2][Ru_3H(\mu_3\text{-}PPh)(CO)_9]$.—Reaction of a solution of (1) in methanol with a slight excess of methanolic KOH at room temperature (r.t.) for 1 h, followed by addition of $[N(PPh_3)_2]Cl$, gives the complex $[N(PPh_3)_2][Ru_3H(\mu_3\text{-}PPh)(CO)_9]$ (2) which was isolated in near quantitative yield as an orange powder. Complex (2) is soluble in dichloromethane but practically insoluble in water and in non-polar organic solvents. It is indefinitely stable in air in the solid state and decomposes only slowly in solution.

The i.r. spectrum of (2) (Table 1) shows, in addition to bands due to terminal CO ligands, a weak broad band at 1 715 cm^{-1} which we assign to a bridging CO group. On this basis, and by analogy with the structure of (1) [1] and a gold derivative (see below), we tentatively propose the structure for (2) shown in Figure 1. A $^{13}C\text{-}\{^1H\}$ n.m.r. spectrum of (2) was recorded at −110 °C in an attempt to confirm the proposed structure but even at this low temperature, below which the complex is too insoluble for a spectrum to be recorded, the cluster is fluxional and a limiting spectrum could not be obtained. Thus four approximately equal intensity resonances are observed in the region δ +215—230 p.p.m. (one of which is a doublet) which may be assigned to terminal CO groups, and there is an additional very broad peak at δ *ca.* 234 which is presumably due to the remaining terminal CO groups exchanging with the bridging CO. A $^{31}P\text{-}\{^1H\}$ n.m.r. spectrum of (2) shows a singlet resonance due to the capping phosphorus atom at δ +153 [relative to $P(OMe)_3$: δ = 0 p.p.m.] which is shifted *ca.* 15 p.p.m. downfield from the corresponding resonance in the spectrum of (1).[1]

Protonation of (2) with an excess of CF_3CO_2H causes the metal–hydride doublet resonance present in the ^1H n.m.r. spectrum of (2) (Table 3) at δ −19.31 to shift to δ −19.56

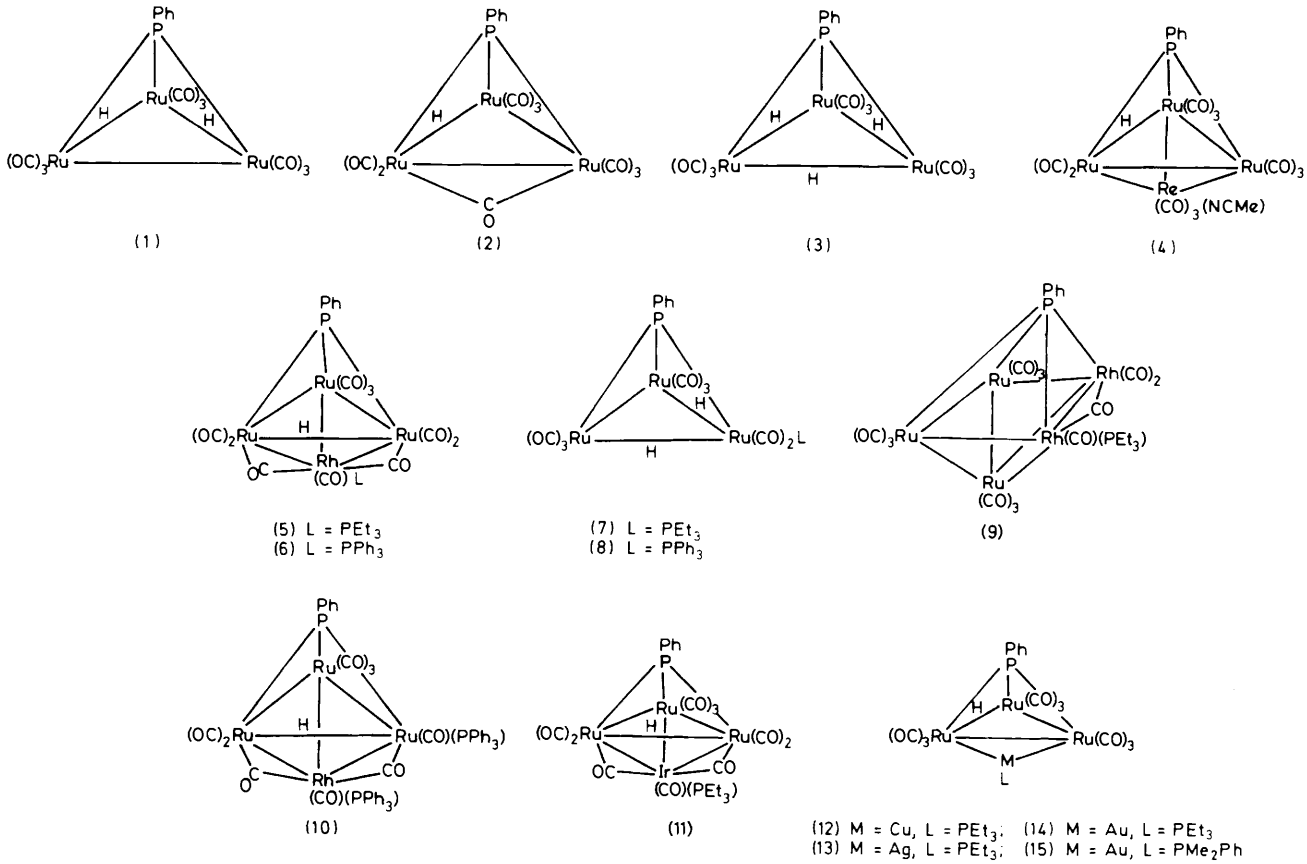

Figure 1. Proposed structures for the triruthenium clusters

p.p.m., and the integrated intensity of this signal with respect to the phenyl H resonances changes from 1 : 5 to 3 : 5. Presumably the protonated complex $[Ru_3(\mu\text{-}H)_3(\mu_3\text{-}PPh)(CO)_9]^+$ (3) is present in solution, and the equivalence of the metal-bound H atoms suggests that it has the structure shown in Figure 1. Extraction of the solution of (3) with dichloromethane–water affords (1) in essentially quantitative yield [δ(RuH) = −19.19 p.p.m.].[1]

It has been reported that it is possible to remove two protons from $[Fe_3H_2(\mu_3\text{-}PPh)(CO)_9]$, on treatment of this complex with $LiBu^n$, to give the dianion $[Fe_3(\mu_3\text{-}PPh)(CO)_9]^{2-}$.[13] Attempts to remove two protons from (1) to give the corresponding ruthenium dianion, however, were unsuccessful. Thus treatment of (1) with a two-fold or greater excess of KOH, $LiBu^n$, NaH, KH, or Na/Hg gave only the monoanion (2).

(*b*) *Synthesis of Mixed-metal Clusters from* (2).—(*i*) *Ruthenium–rhenium.* Reaction of (2) with $[Re(CO)_3(NCMe)_3]BF_4$ in CH_2Cl_2 at r.t. gives, after 1 h, an orange solution from which an orange complex (4) was separated by t.l.c. in *ca.* 40% yield. The highest peak observed in the mass spectrum of this complex (Table 1) was at *m*/*z* = 951 which corresponds to the formulation $[Ru_3ReH(\mu_3\text{-}PPh)(CO)_{11}(NCMe)]$ (4). In accordance with this formulation the ^1H n.m.r. spectrum of (4) shows, in addition to the phenyl resonance of the PPh ligand, a doublet metal hydride resonance at δ −18.65 and a singlet at δ 3.07 which may be assigned to the MeCN group.

The effective atomic number (e.a.n.) rule requires six metal–metal bonds to be present in (4) and a structure which is consistent with the spectroscopic data and with this requirement is shown in Figure 1. A related complex containing three Os and one Re atom has been prepared previously [14] but (4) is, to our knowledge, the first tetranuclear ruthenium–rhenium complex to have been reported.

(*ii*) *Ruthenium–rhodium.* Reaction of (2) with $[Rh(CO)_3(PR_3)_2]^+$ (R = Et or Ph) in CH_2Cl_2 at r.t. gave, in each case, one major and two minor products. The major product for R = Et was a red complex which gave a parent ion in its mass spectrum at *m*/*z* = 916 corresponding to the formulation $[Ru_3RhH(PPh)(CO)_{10}(PEt_3)]$ (5). A mass spectrum could not be obtained for the major product of the reaction with R = Ph, but i.r. and ^1H n.m.r. data show that it is analogous to (5) and should be formulated as $[Ru_3RhH(PPh)(CO)_{10}(PPh_3)]$ (6).

The structures we propose for complexes (5) and (6) are shown in Figure 1, these proposals being supported by the spectroscopic data. Thus the i.r. spectra of (5) and (6) indicate the presence of edge-bridging CO ligands, and a resonance in the $^{13}C\text{-}\{^1H\}$ n.m.r. spectrum of (6) at δ 221.1 of relative intensity 2 can be assigned to such bridging groups. This resonance is split by the rhodium and by the capping phosphorus atom [$J(^{13}C\text{–}^{103}Rh)$ = 32, $^2J(^{13}C\text{–}^{31}P)$ = 16 Hz], these coupling constants being in good agreement with those observed for the CO group bridging the rhodium and an iron atom in $[Rh\{Fe(\mu\text{-}PPh_2)(\eta^5\text{-}C_5H_5)(CO)_2\}_2]$.[15] Five ^{13}CO resonances are observed in the terminal region in an intensity ratio of 2 : 2 : 2 : 1 : 1 as required for the structure shown. That the PPh_3 ligand is bound to rhodium is indicated by the $J(^{31}P\text{–}^{103}Rh)$ coupling constant of 128 Hz and, by the same token, the fact that the capping PPh ligand shows no coupling to rhodium suggests that it remains μ_3-bound to the ruthenium atoms.

One of the minor products of the reaction of (2) with $[Rh(CO)_3(PR_3)_2]^+$ (R = Et or Ph) is a pale yellow complex which has almost the same i.r. spectrum for both R = Et and

Table 1. Mass spectroscopic and i.r. data for new complexes

Compound	Mass spectrum		ν(CO)/cm^{-1} [a]
	M	Fragmentation	
(2) $[N(PPh_3)_2][Ru_3H(\mu_3\text{-}PPh)(CO)_9]$			2 049m, 2 017s, 1 986s, 1 966s, 1 947m, 1 905m, 1 715w br
(3) $[Ru_3H_3(\mu_3\text{-}PPh)(CO)_9]^+$			2 144m, 2 135w, 2 122s, 2 086s, 2 067m, 2 020m
(4) $[Ru_3ReH(\mu_3\text{-}PPh)(CO)_{11}(NCMe)]$	951	*M* − NCMe	2 083m, 2 057s, 2 039s, 2 031s, 2 019m,
		M − NCMe − *n*CO [b]	2 010m, 2 001m, 1 988w
(5) $[Ru_3RhH(\mu_3\text{-}PPh)(CO)_{10}(PEt_3)]$	916	*M* − *n*CO [c]	2 085w, 2 058m, 2 027s, 2 020s, 2 004m, 1 980m, 1 867w br, 1 850w br
(6) $[Ru_3RhH(\mu_3\text{-}PPh)(CO)_{10}(PPh_3)]$			2 088w, 2 062m, 2 034s, 2 024s, 2 001m, 1 983m, 1 869w br, 1 853w br
(7) $[Ru_3H_2(\mu_3\text{-}PPh)(CO)_8(PEt_3)]$			2 074m, 2 043s, 2 037s, 2 005s, 1 991s, 1 982m, 1 970w
(8) $[Ru_3H_2(\mu_3\text{-}PPh)(CO)_8(PPh_3)]$			2 073m, 2 043s, 2 036s, 2 003s, 1 989s, 1 980m, 1 967w
(9) $[Ru_3Rh_2(\mu_4\text{-}PPh)(CO)_{13}(PEt_3)]$	1 102	*M* − *n*CO [d]	2 076m, 2 045s, 2 033s, 2 025s, 2 006m, 1 993m, 1 964w, 1 838w br
(10) $[Ru_3RhH(\mu_3\text{-}PPh)(CO)_9(PPh_3)_2]$			2 065m, 2 043s, 2 035s, 2 013s, 1 981s, 1 953m, 1 837w br, 1 807w br
(11) $[Ru_3IrH(\mu_3\text{-}PPh)(CO)_{10}(PEt_3)]$	1 005	*M* − *n*CO [c]	2 085m, 2 059s, 2 025s, 2 015s, 1 995m, 1 978m, 1 833w (sh), 1 820w br
(12) $[Ru_3\{Cu(PEt_3)\}H(\mu_3\text{-}PPh)(CO)_9]$	848	*M* − *n*CO [e]	2 070m, 2 045s, 2 035m, 2 017s, 1 995m, 1 977m, 1 959m, 1 923w
(13) $[Ru_3\{Ag(PEt_3)\}H(\mu_3\text{-}PPh)(CO)_9]$	892	*M* − *n*CO [e]	2 068m, 2 046s, 2 036m, 2 013s, 1 993m, 1 973m, 1 955m, 1 930w
(14) $[Ru_3\{Au(PEt_3)\}H(\mu_3\text{-}PPh)(CO)_9]$	892	*M* − *n*CO [e]	2 071m, 2 048s, 2 034m, 2 019s, 1 993m, 1 976m, 1 959m, 1 942w
(15) $[Ru_3\{Au(PMe_2Ph)\}H(\mu_3\text{-}PPh)(CO)_9]$	1 002	*M* − *n*CO [e]	2 071m, 2 049s, 2 036m, 2 021s, 1 994m, 1 977m, 1 963m, 1 942w

[a] Recorded in cyclohexane, apart from complexes (2) and (3) which were recorded in CH_2Cl_2. [b] n = 1—11. [c] n = 1—10. [d] n = 1—13. [e] n = 1—9.

Table 2. Carbon-13 n.m.r. data [a] and ^{31}P n.m.r. data [b] for complexes (6) and (10)

Complex	^{13}C n.m.r. (δ/p.p.m.)	^{31}P n.m.r. (δ/p.p.m.)
(6)	221.1 [d of d, J(RhC) = 32, ^2J(PC) = 16, 2 C, μ-CO]	79.3 (s, 1 P, RuP)
	200.5 [d, ^2J(PC) = 30, 1 C, RuCO]	−109.1 [d, J(RhP) = 128, 1 P, RhP]
	200.1 (s, 2 C, RuCO)	
	194.2 (s, 2 C, RuCO)	
	189.6 (s, 2 C, RuCO)	
	181.1 [d of d, J(RhC) = 128, ^2J(P′C) = 22, 1 C, RhCO]	
	133.1—128.5 (m, Ph)	
(10)		54.4 (s, 1 P, μ_3-P)
		−83.2 (s, 1 P, RuP)
		−113.0 [d, J(RhP) = 137, 1 P, RhP]

[a] Recorded at −70 °C in CD_2Cl_2. [b] Recorded at −70 °C in CD_2Cl_2–CH_2Cl_2 (2 : 1); relative to $P(OMe)_3$, δ = 0 p.p.m.

R = Ph. We formulate these complexes as $[Ru_3H_2(\mu_3\text{-}PPh)(CO)_8(PR_3)]$ [R = Et (7); R = Ph (8)] with the structures shown in Figure 1 and, in the case of the phenyl derivative, this structure has been confirmed by an *X*-ray crystal structure investigation.[16] These complexes are probably formed by reaction of free PR_3, liberated from the $[Rh(CO)_3(PR_3)_2]^+$ cation, with (2).

The second minor product of the reaction with R = Et is a green complex (5% yield) which shows a parent ion in its mass spectrum at *m*/*z* 1 102. No metal-bound hydride ligands were seen in the ^{1}H n.m.r. spectrum of the complex, which showed only resonances due to the PPh and a PEt_3 ligand. Dark green crystals suitable for an *X*-ray analysis (see below) were obtained by slow crystallisation from hexane at 0 °C and this analysis reveals that the complex should be formulated as $[Ru_3Rh_2(\mu_4\text{-}PPh)(CO)_{13}(PEt_3)]$ (9).

The molecular structure of (9) is shown in Figure 2 and selected bond lengths and bond angles are given in Tables 4 and 5 respectively. The five metal atoms in the structure of (9) define a square-based pyramid with the μ_4-P atom of the PPh ligand lying 1.23 Å below the square base. The metal geometry observed for (9) has been reported for the structures of $[Os_5(\mu_4\text{-}POMe)(CO)_{15}]$ [17] and for $[Ru_5(\mu_4\text{-}PR)(CO)_{15}]$ (R = Ph or Et).[2] In the structure of (9) the Rh_2Ru_2 basal unit is planar to within ±0.011 Å, with the apical Ru(5) atom 1.966 Å above this plane. The phosphinato P atom bonds fairly symmetrically to the four metal atoms with the mean Rh–P(1) distance of 2.374 Å and the mean Ru–P(1) distance of 2.347 Å. The two Rh atoms occupy adjacent positions in the basal plane with a Rh–Rh distance of 2.775(1) Å, and are bridged by a carbonyl group. The remaining 12 carbonyls are all terminally co-ordinated and essentially linear. The PEt_3 ligand occupies an axial site on Rh(1). Within the molecule the Ru atoms form a nearly regular triangle with Ru–Ru distances of 2.837(1)—2.874(1) Å. The Ru–Rh distances can be divided into two sets with the Rh distances to the capping Ru(5) atom 2.758(1) and 2.783(1) Å] significantly shorter than the Ru–Rh distances within the square base of 2.930(1) and 2.862(1) Å.

Table 3. Hydrogen-1 n.m.r. data for the new complexes

Compound	δ/p.p.m.*
(2)	7.51 (m, 35 H, Ph), −19.31 [d, ^2J(PH) = 16, 1 H, RuH]
(3)	7.75 (m, 5 H, Ph), −19.56 [d, ^2J(PH) = 15, 3 H, RuH]
(4)	7.50 (m, 5 H, Ph), 3.07 (s, 3 H, Me), −18.65 [d, ^2J(PH) = 16, 1 H, RuH]
(5)	8.03 (m, 5 H, Ph), 2.0—1.0 (m, 15 H, Et), −23.67 [d of t, ^2J(PH) = 14, ^2J(RhH) = 14, ^3J(P′H) = 5, 1 H, RuH]
(6)	7.94 (m, 20 H, Ph), −24.40 [d of t, ^2J(PH) = 14, ^2J(RhH) = 14, ^3J(P′H) = 4, 1 H, RuH]
(8)	7.53 (m, 20 H, Ph), −18.54 [d of d, ^2J(PH) = 16, ^2J(P′H) = 10, 2 H, RuH]
(9)	7.45 (m, 5 H, Ph), 2.0—1.0 (m, 15 H, Et)
(10)	7.44 (m, 35 H, Ph), −21.51 [d of q, ^2J(PH) = 14, ^2J(RhH) = 14, ^2J(P′H) = 14, ^3J(P″H) = 4, 1 H, RuH]
(11)	7.84 (m, 5 H, Ph), 2.0—1.0 (m, 15 H, Et), −25.86 [d of d, ^2J(PH) = 15, ^3J(P′H) = 4, 1 H, RuH]
(12)	7.82 (m, 5 H, Ph), 2.2—1.2 (m, 15 H, Et), −20.24 [d, ^2J(PH) = 15, 1 H, RuH]
(13)	7.82 (m, 5 H, Ph), 2.2—1.2 (m, 15 H, Et), −20.52 [d, ^2J(PH) = 15, 1 H, RuH]
(14)	7.82 (m, 5 H, Ph), 2.2—1.2 (m, 15 H, Et), −20.70 [d, ^2J(PH) = 15, 1 H, RuH]
(15)	7.75 (m, 10 H, Ph), 1.84 [d, ^2J(P′H) = 15, 6 H, Me], −20.68 [d, ^2J(PH) = 15, 1 H, RuH]

* Recorded in CD_2Cl_2 at −70 °C. J Values are in Hz; s = singlet, d = doublet, t = triplet, q = quartet, m = multiplet.

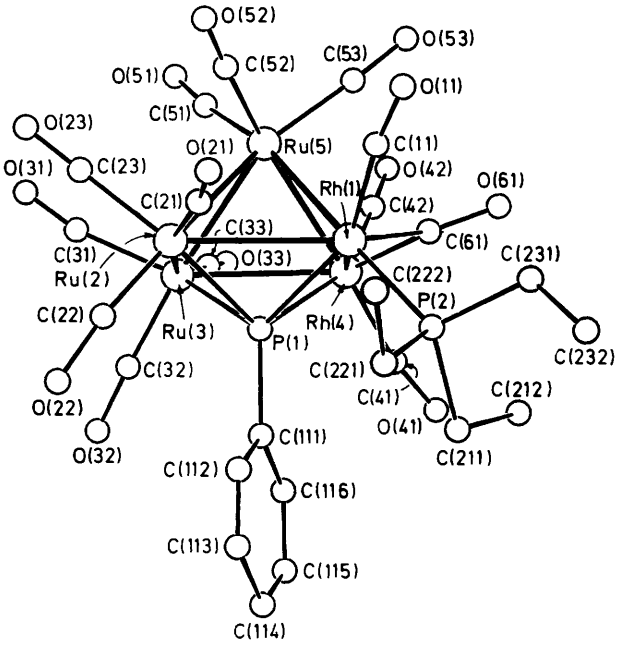

Figure 2. Molecular structure of $[Ru_3Rh_2(\mu_4\text{-PPh})(CO)_{13}(PEt_3)]$ (9) including the atom-numbering scheme

This pattern of M(basal)–M(apical) bonds being shorter than the M(basal)–M(basal) distances is reversed in the structure of $[Os_5(\mu_4\text{-POMe})(CO)_{15}]$, presumably due to differences in the μ_4-POMe and μ_4-PPh ligands.[17] The mean Ru–Ru distance found in (9) (2.855 Å) is the same as the mean Ru–Ru distance found for $[Ru_5(\mu_4\text{-PPh})(CO)_{15}]$ of 2.852 Å.[2]

It seems likely that the formation of (9) in the reaction of (2) with $[Rh(CO)_3(PEt_3)_2]^+$ proceeds *via* (5) as an intermediate. Deprotonation of (5), probably *via* proton exchange with (2) to give (1) and $[Ru_3Rh(\mu_3\text{-PPh})(CO)_{10}(PEt_3)]^-$, followed by reaction of this ruthenium–rhodium anion with a second molecule of $[Rh(CO)_3(PEt_3)_2]^+$, could then give (9). That this is a feasible route was shown in a separate experiment in which (5) was treated with methanolic KOH followed by $[Rh(CO)_3(PEt_3)_2]^+$. The major product isolated from this reaction was (2), but some (9) is also formed. An attempt was made to prepare a complex containing three different transition metals by treating (5) with methanolic KOH as above and then adding one mol of $[Au(PEt_3)_2]PF_6$. In this case, however, only the anion (2) could be isolated.

The formation of complex (9) clearly involves a skeletal rearrangement in which one Ru atom becomes detached from the capping μ_3-PPh ligand present in (2). Such detachment of a bridging or capping phosphorus ligand is unusual but is not without precedent,[8] and provides further evidence that the presence of such ligands does not necessarily prevent cluster fragmentation. Only one other mixed-metal complex containing a μ_4-PPh ligand has been reported [18] and such complexes are of particular interest in view of the observation that the related homometallic complexes $[Co_4(\mu_4\text{-PPh})(CO)_8L_2]$ (L = PPh_3 or CO) are active hydroformylation catalysts.[6]

The second minor product of the reaction of (2) with $[Rh(CO)_3(PPh_3)_2]^+$ is a red complex which we formulate on the basis of spectroscopic data as $[Ru_3RhH(\mu_3\text{-PPh})(CO)_9(PPh_3)_2]$ (10). In accordance with this formulation the ^{31}P n.m.r. spectrum of (10) shows, in addition to a singlet resonance due to the μ_3-PPh ligand, two resonances each of relative intensity 1, one of which is a singlet and the other a doublet [$J(^{31}P–^{103}Rh)$ = 137 Hz]. These must be due, respectively, to PPh_3 ligands terminally bonded to Ru and to Rh. The ^1H n.m.r. spectrum of (10) shows a multiplet phenyl resonance of the relative intensity expected for a capping μ_3-PPh and two PPh_3 ligands. There is also a metal hydride resonance at δ −21.51, of relative intensity 1, which shows coupling to all three phosphorus and the Rh atom. Insufficient material was available for a ^{13}C n.m.r. spectrum to be recorded but we tentatively propose that (10) has the structure shown in Figure 1, this structure being analogous to that of (6) with a terminal CO group on one of the ruthenium atoms being substituted by PPh_3.

(*iii*) *Ruthenium–iridium.* Reaction of (2) with $[Ir(cod)(PEt_3)_2]BF_4$ (cod = cyclo-octa-1,5-diene) in CH_2Cl_2 at r.t. gives two products which were isolated in *ca.* 50% and 14% yield. The major product, a pale yellow complex, was identified spectroscopically as (7). The minor product, a red complex, showed a parent ion peak in its mass spectrum at m/z = 1 005 (^{193}Ir) and its ν(CO) i.r. spectrum and ^1H n.m.r. spectrum are closely similar to those of (5), apart from the absence of the ^{103}Rh–H coupling observed in the ^1H n.m.r. of (5). On this basis it is formulated as $[Ru_3IrH(\mu_3\text{-PPh})(CO)_{10}(PEt_3)]$ (11) with a structure analogous to that of (5), as shown in Figure 1.

(*iv*) *Ruthenium–copper, ruthenium–silver, and ruthenium–gold.* Reaction of (2) with $[\{M(PEt_3)I\}_4]$ (M = Cu or Ag) in CH_2Cl_2 solution at r.t. gives orange solutions from which the orange heterometallic clusters $[Ru_3\{M(PEt_3)\}H(\mu_3\text{-PPh})(CO)_9]$ [M = Cu (12); M = Ag (13)] were isolated by t.l.c. Analogous gold complexes $[Ru_3\{Au(PR_2R')\}H(\mu_3\text{-PPh})(CO)_9]$ [R = R′ = Et (14); R = Me, R′ = Ph (15)] are obtained by

Table 4. Bond lengths (Å) for (9)

Rh(1)–Ru(2)	2.930(1)	Rh(1)–Rh(4)	2.775(1)	Ru(5)–C(53)	1.916(9)	P(1)–C(111)	1.818(6)
Rh(1)–Ru(5)	2.783(1)	Rh(1)–P(1)	2.365(2)	C(111)–C(112)	1.406(11)	C(111)–C(116)	1.403(10)
Rh(1)–P(2)	2.362(2)	Rh(1)–C(11)	1.875(8)	C(112)–C(113)	1.401(12)	C(113)–C(114)	1.372(15)
Rh(1)–C(61)	2.047(7)	Ru(2)–Ru(3)	2.837(1)	C(114)–C(115)	1.380(15)	C(115)–C(116)	1.362(11)
Ru(2)–Ru(5)	2.853(1)	Ru(2)–P(1)	2.340(2)	P(2)–C(211)	1.845(9)	P(2)–C(221)	1.845(9)
Ru(2)–C(21)	1.913(8)	Ru(2)–C(22)	1.889(9)	P(2)–C(231)	1.837(8)	C(211)–C(212)	1.486(13)
Ru(2)–C(23)	1.926(8)	Ru(3)–Rh(4)	2.862(1)	C(221)–C(222)	1.523(13)	C(231)–C(232)	1.539(11)
Ru(3)–Ru(5)	2.874(1)	Ru(3)–P(1)	2.355(2)	C(11)–O(11)	1.132(10)	C(21)–O(21)	1.136(10)
Ru(3)–C(31)	1.903(9)	Ru(3)–C(32)	1.871(9)	C(22)–O(22)	1.123(11)	C(23)–O(23)	1.109(10)
Ru(3)–C(33)	1.900(8)	Rh(4)–Ru(5)	2.758(1)	C(31)–O(31)	1.148(11)	C(32)–O(32)	1.151(11)
Rh(4)–P(1)	2.383(2)	Rh(4)–C(41)	1.944(8)	C(33)–O(33)	1.141(10)	C(41)–O(41)	1.115(10)
Rh(4)–C(42)	1.885(7)	Rh(4)–C(61)	2.081(7)	C(42)–O(42)	1.152(9)	C(51)–O(51)	1.166(10)
Ru(5)–C(51)	1.884(8)	Ru(5)–C(52)	1.907(9)	C(52)–O(52)	1.122(11)	C(53)–O(53)	1.133(12)
				C(61)–O(61)	1.139(9)		

Table 5. Bond angles (°) for (9) *

Rh(4)–Rh(1)–Ru(2)	89.6	Ru(5)–Rh(1)–Ru(2)	59.9	C(42)–Rh(4)–Ru(3)	104.7(2)	C(42)–Rh(4)–Ru(5)	84.8(2)
Ru(5)–Rh(1)–Rh(4)	59.5	P(1)–Rh(1)–Ru(2)	51.1	C(42)–Rh(4)–P(1)	155.5(2)	C(42)–Rh(4)–C(41)	96.2(3)
P(1)–Rh(1)–Rh(4)	54.5	P(1)–Rh(1)–Ru(5)	76.3	C(61)–Rh(4)–Rh(1)	47.2(2)	C(61)–Rh(4)–Ru(3)	136.6(2)
P(2)–Rh(1)–Ru(2)	122.4(1)	P(2)–Rh(1)–Rh(4)	118.0(1)	C(61)–Rh(4)–Ru(5)	82.7(2)	C(61)–Rh(4)–P(1)	98.3(2)
P(2)–Rh(1)–Ru(5)	177.1(1)	P(2)–Rh(1)–P(1)	103.6(1)	C(61)–Rh(4)–C(41)	97.6(3)	C(61)–Rh(4)–C(42)	94.8(3)
C(11)–Rh(1)–Ru(2)	104.5(2)	C(11)–Rh(1)–Rh(4)	133.0(2)	Ru(2)–Ru(5)–Rh(1)	62.6	Ru(3)–Ru(5)–Rh(1)	91.2
C(11)–Rh(1)–Ru(5)	89.2(2)	C(11)–Rh(1)–P(1)	155.5(2)	Ru(3)–Ru(5)–Ru(2)	59.4	Rh(4)–Ru(5)–Rh(1)	60.1
C(11)–Rh(1)–P(2)	91.9(2)	C(61)–Rh(1)–Ru(2)	135.4(2)	Rh(4)–Ru(5)–Ru(2)	91.6	Rh(4)–Ru(5)–Ru(3)	61.1
C(61)–Rh(1)–Rh(4)	48.3(2)	C(61)–Rh(1)–Ru(5)	82.6(2)	C(51)–Ru(5)–Rh(1)	165.8(2)	C(51)–Ru(5)–Ru(2)	113.8(2)
C(61)–Rh(1)–P(1)	99.9(2)	C(61)–Rh(1)–P(2)	94.5(2)	C(51)–Ru(5)–Ru(3)	75.9(2)	C(51)–Ru(5)–Rh(4)	107.4(2)
C(61)–Rh(1)–C(11)	97.6(3)	Ru(3)–Ru(2)–Rh(1)	89.0	C(52)–Ru(5)–Rh(1)	96.0(2)	C(52)–Ru(5)–Ru(2)	75.9(3)
Ru(5)–Ru(2)–Rh(1)	57.5	Ru(5)–Ru(2)–Ru(3)	60.7	C(52)–Ru(5)–Ru(3)	124.6(3)	C(52)–Ru(5)–Rh(4)	156.1(2)
P(1)–Ru(2)–Rh(1)	51.9	P(1)–Ru(2)–Ru(3)	53.1	C(52)–Ru(5)–C(51)	96.2(3)	C(53)–Ru(5)–Rh(1)	92.0(2)
P(1)–Ru(2)–Ru(5)	75.2	C(21)–Ru(2)–Rh(1)	74.5(2)	C(53)–Ru(5)–Ru(2)	149.9(3)	C(53)–Ru(5)–Ru(3)	142.5(3)
C(21)–Ru(2)–Ru(3)	161.5(2)	C(21)–Ru(2)–Ru(5)	102.4(2)	C(53)–Ru(5)–Rh(4)	88.8(3)	C(53)–Ru(5)–C(51)	94.7(4)
C(21)–Ru(2)–P(1)	118.2(2)	C(22)–Ru(2)–Rh(1)	127.1(3)	C(53)–Ru(5)–C(52)	92.1(4)	Ru(2)–P(1)–Rh(1)	77.0(1)
C(22)–Ru(2)–Ru(3)	99.4(3)	C(22)–Ru(2)–Ru(5)	160.0(3)	Ru(3)–P(1)–Rh(1)	117.8(1)	Ru(3)–P(1)–Ru(2)	74.4
C(22)–Ru(2)–P(1)	93.1(3)	C(22)–Ru(2)–C(21)	97.4(4)	Rh(4)–P(1)–Rh(1)	71.5	Rh(4)–P(1)–Ru(2)	116.7(1)
C(23)–Ru(2)–Rh(1)	140.8(3)	C(23)–Ru(2)–Ru(3)	91.9(2)	Rh(4)–P(1)–Ru(3)	74.3	C(111)–P(1)–Rh(1)	121.5(2)
C(23)–Ru(2)–Ru(5)	89.3(2)	C(23)–Ru(2)–P(1)	144.9(2)	C(111)–P(1)–Ru(2)	122.0(2)	C(111)–P(1)–Ru(3)	120.6(2)
C(23)–Ru(2)–C(21)	95.6(3)	C(23)–Ru(2)–C(22)	91.4(4)	C(111)–P(1)–Rh(4)	121.3(2)	C(112)–C(111)–P(1)	120.6(5)
Rh(4)–Ru(3)–Ru(2)	89.7	Ru(5)–Ru(3)–Ru(2)	59.9	C(116)–C(111)–P(1)	120.3(5)	C(116)–C(111)–C(112)	119.1(6)
Ru(5)–Ru(3)–Rh(4)	57.5	P(1)–Ru(3)–Ru(2)	52.6	C(113)–C(112)–C(111)	118.3(8)	C(114)–C(113)–C(112)	120.9(9)
P(1)–Ru(3)–Rh(4)	53.3	P(1)–Ru(3)–Ru(5)	74.6	C(115)–C(114)–C(113)	120.5(8)	C(116)–C(115)–C(114)	119.8(9)
C(31)–Ru(3)–Ru(2)	89.5(3)	C(31)–Ru(3)–Rh(4)	150.5(3)	C(115)–C(116)–C(111)	121.3(8)	C(211)–P(2)–Rh(1)	117.9(3)
C(31)–Ru(3)–Ru(5)	97.3(3)	C(31)–Ru(3)–P(1)	140.5(3)	C(221)–P(2)–Rh(1)	116.3(3)	C(221)–P(2)–C(211)	101.8(4)
C(32)–Ru(3)–Ru(2)	109.1(3)	C(32)–Ru(3)–Rh(4)	117.5(3)	C(231)–P(2)–Rh(1)	111.2(2)	C(231)–P(2)–C(211)	104.0(4)
C(32)–Ru(3)–Ru(5)	166.3(3)	C(32)–Ru(3)–P(1)	92.2(3)	C(231)–P(2)–C(221)	104.1(4)	C(212)–C(211)–P(2)	115.1(6)
C(32)–Ru(3)–C(31)	90.5(4)	C(33)–Ru(3)–Ru(2)	156.5(2)	C(222)–C(221)–P(2)	116.2(6)	C(232)–C(231)–P(2)	116.3(6)
C(33)–Ru(3)–Rh(4)	73.2(2)	C(33)–Ru(3)–Ru(5)	96.9(2)	O(11)–C(11)–Rh(1)	176.4(7)	O(21)–C(21)–Ru(2)	173.9(7)
C(33)–Ru(3)–P(1)	121.7(2)	C(33)–Ru(3)–C(31)	97.5(3)	O(22)–C(22)–Ru(2)	177.6(8)	O(23)–C(23)–Ru(2)	176.9(7)
C(33)–Ru(3)–C(32)	93.3(4)	Ru(3)–Rh(4)–Rh(1)	91.6	O(31)–C(31)–Ru(3)	176.9(8)	O(32)–C(32)–Ru(3)	178.5(9)
Ru(5)–Rh(4)–Rh(1)	60.4	Ru(5)–Rh(4)–Ru(3)	61.5	O(33)–C(33)–Ru(3)	173.9(7)	O(41)–C(41)–Rh(4)	175.6(7)
P(1)–Rh(4)–Rh(1)	53.9	P(1)–Rh(4)–Ru(3)	52.4	O(42)–C(42)–Rh(4)	179.2(7)	O(51)–C(51)–Ru(5)	174.8(7)
P(1)–Rh(4)–Ru(5)	76.5	C(41)–Rh(4)–Rh(1)	119.0(2)	O(52)–C(52)–Ru(5)	173.4(8)	O(53)–C(53)–Ru(5)	175.5(8)
C(41)–Rh(4)–Ru(3)	117.8(2)	C(41)–Rh(4)–Ru(5)	178.9(2)	Rh(4)–C(61)–Rh(1)	84.5(3)	O(61)–C(61)–Rh(1)	139.2(6)
C(41)–Rh(4)–P(1)	102.4(2)	C(42)–Rh(4)–Rh(1)	128.2(2)	O(61)–C(61)–Rh(4)	136.3(6)		

* E.s.d.s. have been rounded to one decimal place and, where not given, are less than 0.05 °.

reaction of (2) with $[Au(PR_2R')_2]PF_6$ under the same conditions. Complexes (12)—(15) all show parent ion peaks in their mass spectra and the i.r. and ^1H n.m.r. of the four complexes are virtually identical apart from the observation of an ^1H n.m.r. resonance due to the Me groups in (15). The structure of (15) has been determined by an *X*-ray analysis (see below) and the structures of the other three complexes (Figure 1) are presumably analogous.

The molecular structure of $[Ru_3\{\mu\text{-}Au(PMe_2Ph)\}(\mu\text{-}H)(\mu_3\text{-}PPh)(CO)_9]$ (15) is shown in Figure 3, while the relevant bond lengths and interbond angles are presented in Tables 6 and 7, respectively. In the solid state, molecules of (15) exist as discrete units separated by normal van der Waals distances. Within each molecule the three Ru atoms define an irregular triangle, the longest edge of which [Ru(1)–Ru(2)] is symmetrically bridged by the Au(1) atom of the $Au(PMe_2Ph)$ group. The Au(1)Ru(1)Ru(2) plane makes an angle of 73.8° with the Ru(1)Ru(2)Ru(3) triangle. The Ru_3 triangle is also asymmetrically capped, on the opposite side to the $Au(PMe_2Ph)$ unit, by the P(1) atom of the PPh group; the P(1) atom lies 1.54 Å from the Ru_3 plane. Although the hydride ligand was not located directly in the *X*-ray analysis an

analysis of the distribution of the carbonyl ligands indicates that it bridges the Ru(1)–Ru(3) edge. The *cis*-Ru–Ru–C(carbonyl) angles adjacent to this edge are significantly wider [average 114(3)°] than those adjacent to the unbridged Ru(2)–Ru(3) edge [average 96(1)°] indicating that the steric requirements of the hydride cause the carbonyls to bend back. The nine carbonyl groups are all terminally co-ordinated, three to each Ru atom; and are essentially linear. The rather high estimated standard deviations on the carbonyl C and O atom positions make an accurate assessment of the bonding difficult, but the average Ru–C and C–O bond lengths of 1.91(4) and 1.15(4) Å are close to the expected values.

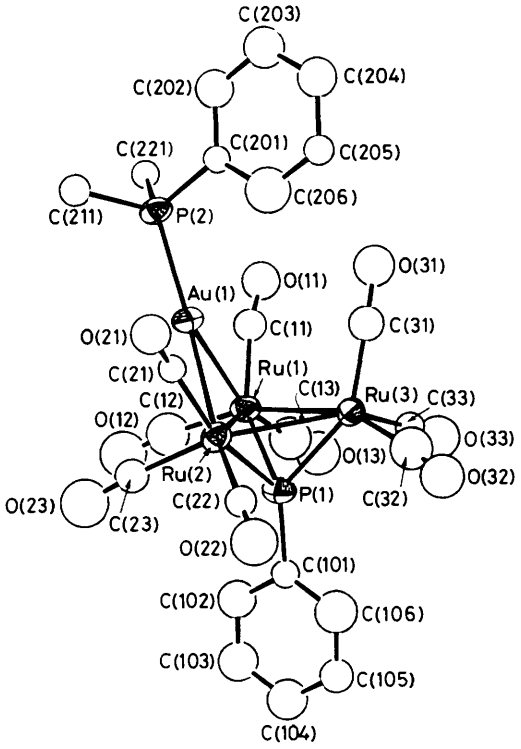

Figure 3. Molecular structure of $[Ru_3\{Au(PMe_2Ph)\}(\mu\text{-}H)(\mu_3\text{-}PPh)(CO)_9]$ (15) including the atom-numbering scheme

This structure allows a comparison of the bonding ability of a hydride and an $Au(PR_3)$ unit, where the Au atom is considered to be in the −1 oxidation state and may be thought of as being *sp* hybridised. Both these ligands are formally two-electron donors. It has been stated that the bonding characteristic of a μ-H and a μ-$Au(PR_3)$ are similar,[19] and there are a number of known structures where the replacement of a hydride by a bridging gold phosphine has little effect on the cluster core or overall geometry.[20] In the case of (15) there is a significant difference in the lengths of the two Ru–Ru bonds which are bridged by the hydride and by the $Au(PR_3)$ unit, the latter being *ca.* 0.03 Å longer. This suggests that, at least in this case, the gold phosphine exerts a greater bond-lengthening influence. Both these Ru–Ru bonds are longer than the third Ru(2)–Ru(3) edge which is only capped by the μ_3-PPh group. This Ru(2)–Ru(3) bond is similar in length to the Ru–Ru bond which is not bridged by a hydride in the related cluster $[Ru_3(\mu\text{-}H)_2\{\mu_3\text{-}P(C_6H_4OMe\text{-}p)\}(CO)_9]$,[2] where the value is 2.844(2) Å. The hydride bridged Ru(1)–Ru(3) bond is slightly longer than the values for equivalent bonds in $[Ru_3(\mu\text{-}H)_2\{\mu_3\text{-}P(C_6H_4OMe\text{-}p)\}(CO)_9]$ [2.933(4) Å][2] and $[Ru_3(\mu\text{-}H)(\mu_3\text{-}PPh)(CO)_8(PPh_3)]$ [2.959(1) Å].[16] The two Au–Ru distances in (15) are similar to the mean value of

Table 6. Bond lengths (Å) for (15)

Ru(1)–Ru(2)	3.002(6)	Ru(1)–Ru(3)	2.972(6)
Ru(1)–Au(1)	2.749(5)	Ru(1)–P(1)	2.347(12)
Ru(1)–C(11)	1.929(35)	Ru(1)–C(12)	1.949(45)
Ru(1)–C(13)	1.881(37)	Ru(2)–Ru(3)	2.869(6)
Ru(2)–Au(1)	2.763(5)	Ru(2)–P(1)	2.258(12)
Ru(2)–C(21)	1.924(40)	Ru(2)–C(22)	1.917(52)
Ru(2)–C(23)	1.911(60)	Ru(3)–P(1)	2.279(11)
Ru(3)–C(31)	1.864(43)	Ru(3)–C(32)	1.838(42)
Ru(3)–C(33)	1.969(52)	Au(1)–P(2)	2.314(9)
P(1)–C(101)	1.794(26)	C(11)–O(11)	1.195(44)
C(12)–O(12)	1.156(60)	C(13)–O(13)	1.150(49)
C(21)–O(21)	1.161(49)	C(22)–O(22)	1.110(64)
C(23)–O(23)	1.110(74)	C(31)–O(31)	1.239(51)
C(32)–O(32)	1.153(53)	C(33)–O(33)	1.119(61)
P(2)–C(201)	1.824(28)	P(2)–C(211)	1.857(40)
P(2)–C(221)	1.830(39)		

Table 7. Bond angles (°) for (15)

Ru(2)–Ru(1)–Ru(3)	57.4(1)	Ru(2)–Ru(1)–Au(1)	57.2(1)	Ru(2)–Ru(3)–P(1)	50.5(3)	Ru(1)–Ru(3)–C(31)	108.6(13)
Ru(3)–Ru(1)–Au(1)	84.6(1)	Ru(2)–Ru(1)–P(1)	48.1(3)	Ru(2)–Ru(3)–C(31)	96.5(14)	P(1)–Ru(3)–C(31)	145.5(14)
Ru(3)–Ru(1)–P(1)	49.0(3)	Au(1)–Ru(1)–P(1)	104.5(3)	Ru(1)–Ru(3)–C(32)	149.9(14)	Ru(2)–Ru(3)–C(32)	96.4(14)
Ru(2)–Ru(1)–C(11)	120.0(11)	Ru(3)–Ru(1)–C(11)	118.6(12)	P(1)–Ru(3)–C(32)	99.4(14)	C(31)–Ru(3)–C(32)	93.5(18)
Au(1)–Ru(1)–C(11)	62.8(11)	P(1)–Ru(1)–C(11)	164.9(11)	Ru(1)–Ru(3)–C(33)	102.8(16)	Ru(2)–Ru(3)–C(33)	157.1(15)
Ru(2)–Ru(1)–C(12)	90.0(12)	Ru(3)–Ru(1)–C(12)	142.4(12)	P(1)–Ru(3)–C(33)	106.9(15)	C(31)–Ru(3)–C(33)	104.9(20)
Au(1)–Ru(1)–C(12)	93.0(11)	P(1)–Ru(1)–C(12)	96.2(12)	C(32)–Ru(3)–C(33)	90.4(20)	Ru(1)–Au(1)–Ru(2)	66.0(1)
C(11)–Ru(1)–C(12)	92.7(16)	Ru(2)–Ru(1)–C(13)	139.2(12)	Ru(1)–Au(1)–P(2)	146.6(3)	Ru(2)–Au(1)–P(2)	146.2(3)
Ru(3)–Ru(1)–C(13)	96.4(13)	Au(1)–Ru(1)–C(13)	159.5(12)	C(11)–Au(1)–P(2)	104.5(8)	C(21)–Au(1)–P(2)	104.6(9)
P(1)–Ru(1)–C(13)	91.3(12)	C(11)–Ru(1)–C(13)	99.5(16)	Ru(1)–P(1)–Ru(2)	81.3(3)	Ru(1)–P(1)–Ru(3)	79.9(3)
C(12)–Ru(1)–C(13)	98.4(17)	Ru(1)–Ru(2)–Ru(3)	60.8(1)	Ru(2)–P(1)–Ru(3)	78.5(3)	Ru(1)–P(1)–C(101)	127.3(10)
Ru(1)–Ru(2)–Au(1)	56.8(1)	Ru(3)–Ru(2)–Au(1)	86.3(1)	Ru(2)–P(1)–C(101)	134.7(10)	Ru(3)–P(1)–C(101)	134.4(9)
Ru(1)–Ru(2)–P(1)	50.6(3)	Ru(3)–Ru(2)–P(1)	51.1(3)	P(1)–C(101)–C(102)	116.1(8)	P(1)–C(101)–C(106)	123.9(8)
Au(1)–Ru(2)–P(1)	106.5(3)	Ru(1)–Ru(2)–C(21)	118.9(12)	Ru(1)–C(11)–O(11)	162.4(32)	Ru(1)–C(12)–O(12)	174.2(37)
Ru(3)–Ru(2)–C(21)	100.4(14)	Au(1)–Ru(2)–C(21)	65.1(12)	Ru(1)–C(13)–O(13)	177.2(35)	Ru(2)–C(21)–O(21)	166.3(36)
P(1)–Ru(2)–C(21)	151.5(14)	Ru(1)–Ru(2)–C(22)	141.8(15)	Ru(2)–C(22)–O(22)	174.9(48)	Ru(2)–C(23)–O(23)	169.6(49)
Ru(3)–Ru(2)–C(22)	96.2(18)	Au(1)–Ru(2)–C(22)	158.7(16)	Ru(3)–C(31)–O(31)	168.7(35)	Ru(3)–C(32)–O(32)	170.6(41)
P(1)–Ru(2)–C(22)	91.2(16)	C(21)–Ru(2)–C(22)	93.7(19)	Ru(3)–C(33)–O(33)	171.9(46)	Au(1)–P(2)–C(201)	112.3(8)
Ru(1)–Ru(2)–C(23)	97.6(16)	Ru(3)–Ru(2)–C(23)	154.5(16)	Au(1)–P(2)–C(211)	117.0(12)	C(201)–P(2)–C(211)	102.4(15)
Au(1)–Ru(2)–C(23)	92.6(15)	P(1)–Ru(2)–C(23)	105.5(16)	Au(1)–P(2)–C(221)	114.5(12)	C(201)–P(2)–C(221)	106.1(15)
C(21)–Ru(2)–C(23)	102.1(21)	C(22)–Ru(2)–C(23)	93.9(24)	C(211)–P(2)–C(221)	103.3(17)	P(2)–C(201)–C(202)	121.1(7)
Ru(1)–Ru(3)–Ru(2)	61.8(1)	Ru(1)–Ru(3)–P(1)	51.0(3)	P(2)–C(201)–C(206)	118.9(7)		

2.761(2) Å observed for the Au–Ru bonds in $[Ru_3\{\mu\text{-}Au(PPh_3)\}(\mu\text{-}COMe)(CO)_{10}]$.[21] The variation in μ-P–Ru distances in (15) is slightly greater than that observed in $[Ru_3(\mu\text{-}H)_2\{\mu_3\text{-}P(C_6H_4OMe\text{-}p)\}(CO)_9]$,[2] where the range is 2.273(4)—2.320(4) Å, but the trend in both compounds is the same in that the longest μ_3-P–Ru distance is to the metal atom involved in bonding with both doubly bridging groups.

Related triruthenium complexes containing up to three edge-bridging $Au(PR_3)$ ligands are known,[22] and it was of interest to determine whether proton abstraction from (14) or (15), followed by addition of a further mole of $[Au(PR_3)_2]PF_6$, would prove to be a viable route to Ru_3Au_2 clusters. Treatment of (14) with stoicheiometric quantities of KOH in methanol or other proton-abstracting agents in tetrahydrofuran solution followed by a mole of $[Au(PEt_3)_2]PF_6$ did not, however, give the desired product. Instead, the anion (2) and some starting material were recovered. It seems, therefore, that the heterometallic complexes described in this paper are less easy to deprotonate than the parent homometallic complex (1). The isolation of the anion (2) as the major product in the reactions of (7) and (14) with base suggests, as a reason, that loss of the heterometal fragment is favoured over deprotonation.

Experimental

All reactions were performed under dry, oxygen-free nitrogen in nitrogen-saturated solvents. Solvents were dried over 4 Å molecular sieves unless otherwise stated. Infrared spectra were recorded in cyclohexane solution with 0.5-mm NaCl cells on a Perkin-Elmer 257 spectrometer using CO gas as calibrant. Mass spectra were obtained on an A.E.I. MS 12 instrument using tris(perfluoroheptyl)-s-triazine as reference. Hydrogen-1 n.m.r. spectra were recorded on Varian Associates XL-100 or Xl-100A 12/12 or Brucker WM250 spectrometers. Carbon-13 and phosphorus-31 n.m.r. spectra were recorded using a Brucker WM250 spectrometer. Microanalysis were carried out at the Chemical Laboratory, Cambridge.

Preparative t.l.c. was performed on silica and products eluted are presented in order of decreasing R_f values.

All chemicals were used as purchased from commercial sources unless otherwise stated. $[Ru_3H_2(\mu_3\text{-}PPh)(CO)_9]$,[1] $[Re(CO)_3(NCMe)_3]BF_4$,[23] $[Rh(CO)_3(PR_3)_2]BF_4$ (R = Et or Ph),[24] $[Ir(cod)(PEt_3)_2]BF_4$,[25] $[\{CuI(PEt_3)\}_4]$,[26] $[\{AgI(PEt_3)\}_4]$,[27] and $[Au(PR_2R')_2]PF_6$ (R = R′ = Et; R = Me, R′ = Ph) [28] were prepared according to literature methods.

(*i*) *Preparation of* $[N(PPh_3)_2][Ru_3H(\mu_3\text{-}PPh)(CO)_9]$ (2).—A solution of (1) (0.05 g, 0.075 mmol) in methanol (20 cm³) was stirred at r.t. with a solution of KOH (0.005 g, 0.089 mmol) in methanol (2 cm³) for 1 h. $[N(PPh_3)_2]Cl$ (0.043 g, 0.075 mmol) was added followed by water (20 cm³) and the mixture was then extracted with CH_2Cl_2 (20 cm³). The organic layer was separated and dried with $MgSO_4$. Filtration, followed by removal of the solvent on a rotary evaporator gave (2) as a dark orange powder (0.083 g, 89%) (Found: C, 51.7; H, 3.4; N, 1.1; P, 7.4. Calc. for $C_{51}H_{36}NO_9P_3Ru_3$: C, 50.9; H, 3.0; N, 1.2; P, 7.7%).

(*ii*) *Preparation of Heterometallic Clusters.*—(*a*) *With rhenium.* To a solution of (2) (0.025 g, 0.021 mmol) in CH_2Cl_2 was added a solution of $[Re(CO)_3(NCMe)_3]BF_4$ (0.211 g, 0.021 mmol) in CH_2Cl_2 (20 cm³) and the mixture stirred at r.t. for 1 h. The solvent was evaporated under reduced pressure and the residue redissolved in a minimum quantity of CH_2Cl_2. This solution was chromatographed using CH_2Cl_2–hexane (1 : 9) as eluant to give (4) on evaporation of the solvent as an orange powder (0.008 g, 40%).

(*b*) *With rhodium.* To a solution of (2) (0.025 g, 0.021 mmol) in CH_2Cl_2 (25 cm³) was added a solution of $[Rh(CO)_3(PR_3)_2]BF_4$ (R = Et, 0.011 g, 0.022 mmol; R = Ph, 0.017 g, 0.022 mmol) in CH_2Cl_2 (20 cm³) and the mixture stirred at r.t. for 1 h. The products were separated by preparative t.l.c. as in (*a*) to give (with R = Et) (7) (0.002 g, 13%), (5) (0.012 g, 63%), and (9) (0.001 g, 4%); or (with R = Ph) (8) (0.002 g, 11%), (6) (0.013 g, 59%), and (10) (0.004 g, 15%) [Found for (9): C, 28.6; H, 1.6; P, 6.5. Calc. for $C_{25}H_{20}O_{13}P_2Rh_2Ru_3$: C, 27.3; H, 1.8; P, 5.6%].

(*c*) *With iridium.* To a solution of (2) (0.025 g, 0.021 mmol) in CH_2Cl_2 (25 cm³) was added a solution of $[Ir(cod)(PEt_3)_2]BF_4$ (0.013 g, 0.021 mmol) in CH_2Cl_2 (20 cm³) and the mixture stirred at r.t. for 1 h. The products were separated by preparative t.l.c. as in (*a*) to give (7) (0.008 g, 50%) and (11) (0.003 g, 14%).

(*d*) *With copper, silver, and gold.* To a solution of (2) (0.025 g, 0.021 mmol) in CH_2Cl_2 (25 cm³) was added a solution of $[\{CuI(PEt_3)\}_4]$ (0.026 g, 0.021 mmol), $[\{AgI(PEt_3)\}_4]$ (0.03 g, 0.021 mmol), $[Au(PEt_3)_2]PF_6$ (0.012 g, 0.021 mmol) or $[Au(PMe_2Ph)_2]PF_6$ (0.013 g, 0.021 mmol) in CH_2Cl_2 (25 cm³) and the mixture stirred at r.t. for 1 h. The product in each case was separated by preparative t.l.c. as in (*a*) to give, respectively, (12) (0.007 g, 39%), (13) (0.008 g, 43%), (14) (0.014 g, 68%), and (15) (0.013 g, 62%) [Found for (15): C, 28.6; H, 1.8; P, 6.0. Calc. for $C_{23}H_{17}AuO_9P_2Ru_3$: C, 27.6; H, 1.7; P, 6.2%].

(*iii*) *Attempted Deprotonation of the Heterometallic Clusters.*—(*a*) *Ruthenium–rhodium.* A solution of (7) (0.020 g, 0.022 mmol) in methanol (20 cm³) was stirred with a solution of KOH (0.002 g, 0.036 mmol) in methanol (10 cm³) for 0.5 h. A solution of $[Rh(CO)_3(PEt_3)_2]BF_4$ (0.011 g, 0.022 mmol) in methanol was added and the mixture stirred for a further 0.5 h. Water (20 cm³) was added and, after extraction of the mixture with CH_2Cl_2 (20 cm³), the organic layer was separated and dried with $MgSO_4$. An i.r. spectrum at this stage showed that the major component present in solution was (2) but separation of the products by t.l.c. using CH_2Cl_2–hexane (1 : 9) as eluant gave, in addition to (2) (0.015 g, 0.013 mmol), a low yield of (9) (0.001 g, 4%).

An identical experiment using $[Au(PEt_3)_2]PF_6$ (0.013 g, 0.023 mmol) in place of $[Rh(CO)_3(PEt_3)_2]BF_4$ gave only (2).

(*b*) *Ruthenium–gold.* A solution of (14) (0.020 g, 0.020 mmol) in methanol (20 cm³) was stirred with a solution of KOH (0.001 g, 0.018 mmol) in methanol (10 cm³) for 0.5 h. A solution of $[Au(PEt_3)_2]PF_6$ (0.011 g, 0.019 mmol) in methanol (10 cm³) was then added and the mixture stirred for a further 0.5 h. Water (20 cm³) was added and after extraction of the mixture with CH_2Cl_2 (20 cm³) the organic layer was separated and dried with $MgSO_4$. An i.r. spectrum at this stage showed only bands due to (2) and t.l.c. did not reveal the presence of any other products.

Crystal Data.—*For* (9). $C_{25}H_{20}O_{13}P_2Rh_2Ru_3$, M = 1 099.49, monoclinic, space group $C2/c$, a = 20.257(5), b = 9.679(3), c = 34.726(5) Å, β = 90.24(2)°, U = 6 808.6 Å³, Z = 8, D_c = 2.145 g cm⁻³, $F(000)$ = 4 216, λ(Mo-K_α) = 0.710 69 Å, μ(Mo-K_α) = 21.83 cm⁻¹.

For (15). $C_{23}H_{17}AuO_9P_2Ru_3$, M = 999.51, monoclinic, space group $P2_1/c$, a = 8.805(3), b = 20.195(7), c = 16.683(6) Å, β = 100.62(2)°, U = 2 915.7 Å³, Z = 4, D_c = 2.276 g cm⁻³, $F(000)$ = 1 872, λ(Mo-K_α) = 0.710 69 Å, μ(Mo-K_α) = 66.18 cm⁻¹.

Intensity Measurements.—*For* (9). Data were collected with a crystal of dimensions *ca.* 0.26 × 0.20 × 0.10 mm on a Philips PW1100 four-circle diffractometer with Mo-K_α radiation from a graphite monochromator. A θ—2θ scan mode was used with a constant scan speed of 0.5° s⁻¹, a scan

Table 8. Fractional atomic co-ordinates for (9)

Atom	*x*	*y*	*z*	Atom	*x*	*y*	*z*
Rh(1)	0.292 61(2)	−0.051 45(5)	0.338 06(1)	C(22)	0.311 6(4)	−0.321 7(8)	0.437 2(2)
Ru(2)	0.354 21(2)	−0.228 78(5)	0.396 37(2)	O(22)	0.287 8(3)	−0.375 1(7)	0.462 2(2)
Ru(3)	0.396 33(2)	0.011 73(6)	0.436 20(2)	C(23)	0.436 1(3)	−0.322 4(8)	0.407 3(2)
Rh(4)	0.337 07(2)	0.179 70(5)	0.377 68(2)	O(23)	0.481 9(3)	−0.381 6(6)	0.413 1(2)
Ru(5)	0.425 90(2)	−0.021 26(6)	0.355 87(2)	C(31)	0.469 9(4)	−0.088 4(9)	0.456 0(2)
P(1)	0.293 74(7)	−0.025 63(17)	0.405 78(5)	O(31)	0.515 1(3)	−0.143 5(7)	0.468 8(2)
C(111)	0.217 7(3)	−0.023 2(7)	0.433 4(1)	C(32)	0.357 8(4)	0.014 3(9)	0.485 1(2)
C(112)	0.199 7(3)	0.094 7(8)	0.454 6(2)	O(32)	0.334 2(3)	0.019 0(9)	0.515 1(1)
C(113)	0.139 2(4)	0.093 5(10)	0.474 0(2)	C(33)	0.432 4(3)	0.191 8(8)	0.441 8(2)
C(114)	0.100 7(4)	−0.023 1(12)	0.474 7(3)	O(33)	0.455 8(3)	0.296 5(6)	0.448 4(1)
C(115)	0.118 3(3)	−0.138 5(11)	0.453 7(2)	C(41)	0.273 5(3)	0.318 7(7)	0.393 6(2)
C(116)	0.176 1(3)	−0.139 1(8)	0.433 8(2)	O(41)	0.240 3(3)	0.404 2(6)	0.402 9(2)
P(2)	0.179 05(8)	−0.064 60(20)	0.322 72(5)	C(42)	0.403 9(3)	0.304 7(7)	0.363 3(2)
C(211)	0.122 1(3)	0.050 7(9)	0.348 8(2)	O(42)	0.444 6(3)	0.382 1(6)	0.354 9(2)
C(212)	0.132 7(4)	0.200 8(10)	0.342 3(3)	C(51)	0.507 9(3)	0.023 0(8)	0.378 6(2)
C(221)	0.139 5(4)	−0.234 5(9)	0.329 4(2)	O(51)	0.560 7(2)	0.049 0(7)	0.389 9(1)
C(222)	0.161 2(5)	−0.348 6(9)	0.302 0(3)	C(52)	0.453 8(3)	−0.190 0(8)	0.332 7(2)
C(231)	0.164 2(3)	−0.023 8(8)	0.271 8(2)	O(52)	0.473 0(3)	−0.281 8(6)	0.316 5(2)
C(232)	0.091 6(4)	−0.024 0(10)	0.258 4(2)	C(53)	0.441 9(4)	0.080 9(10)	0.309 6(2)
C(11)	0.316 3(3)	−0.131 5(8)	0.291 0(2)	O(53)	0.455 3(3)	0.137 4(8)	0.282 1(2)
O(11)	0.331 5(3)	−0.173 1(6)	0.261 8(1)	C(61)	0.301 8(3)	0.151 0(7)	0.321 9(2)
C(21)	0.327 3(3)	−0.350 5(7)	0.355 9(2)	O(61)	0.293 2(2)	0.218 6(5)	0.295 5(1)
O(21)	0.314 4(3)	−0.431 7(5)	0.333 5(1)				

Table 9. Atomic co-ordinates (× 10^4) for (15)

Atom	*X*/*a*	*Y*/*b*	*Z*/*c*	Atom	*X*/*a*	*Y*/*b*	*Z*/*c*
Ru(1)	4 459(5)	4 428(2)	3 068(2)	C(22)	5 579(64)	2 195(27)	3 579(32)
Ru(2)	4 407(5)	2 942(2)	3 100(2)	O(22)	6 332(44)	1 772(18)	3 820(21)
Ru(3)	6 928(4)	3 607(2)	2 570(2)	C(23)	2 846(64)	2 841(26)	3 749(32)
Au(1)	2 494(2)	3 688(1)	1 942(1)	O(23)	2 014(45)	2 871(18)	4 173(23)
P(1)	6 151(12)	3 650(7)	4 799(6)	C(31)	6 348(50)	3 400(21)	1 467(26)
C(101)	7 138(23)	3 710(13)	4 838(17)	O(31)	5 905(36)	3 154(15)	784(19)
C(102)	6 285(23)	3 532(13)	5 431(17)	C(32)	8 307(49)	2 917(21)	2 771(24)
C(103)	6 961(23)	3 561(13)	6 255(17)	O(32)	9 021(41)	2 443(17)	2 947(21)
C(104)	8 491(23)	3 768(13)	6 486(17)	C(33)	8 645(60)	4 239(25)	2 623(29)
C(105)	9 344(23)	3 946(13)	5 893(17)	O(33)	9 568(38)	4 627(16)	2 731(19)
C(106)	8 668(23)	3 917(13)	5 069(17)	P(2)	785(11)	3 681(6)	709(5)
C(11)	3 065(44)	4 903(18)	2 237(22)	C(201)	1 722(22)	3 897(12)	−143(16)
O(11)	2 495(34)	5 326(14)	1 777(17)	C(202)	996(22)	3 781(12)	−947(16)
C(12)	3 015(47)	4 453(20)	3 823(24)	C(203)	1 746(22)	3 943(12)	−1 588(16)
O(12)	2 258(43)	4 491(17)	4 318(22)	C(204)	3 222(22)	4 220(12)	−1 425(16)
C(13)	5 748(46)	5 131(19)	3 510(23)	C(205)	3 949(22)	4 335(12)	−621(16)
O(13)	6 484(40)	5 576(16)	3 778(20)	C(206)	3 199(22)	4 174(12)	20(16)
C(21)	3 531(50)	2 471(20)	2 122(26)	C(211)	−853(44)	4 282(19)	591(22)
O(21)	3 217(35)	2 092(15)	1 594(17)	C(221)	−177(43)	2 887(18)	445(21)

width of 0.8°, and reflections with $3.0 < \theta < 25.0°$ were examined, using the technique previously described.[29] The variance of the intensity (I) was calculated as $\{[\sigma_c(I)]^2 + (0.04I)^2\}^{\frac{1}{2}}$, where $[\sigma_c(I)]$ is the variance due to counting statistics, and the term in I^2 was introduced to allow for other sources of error. Lorentz polarisation corrections were applied and equivalent reflections averaged to give 4 708 unique observed reflections [$F > 6\sigma(F)$]. No absorption correction was applied.

For (15). A yellow, needle shaped single crystal (*ca.* 0.33 × 0.03 × 0.02 mm) was mounted on a glass fibre, and cell dimensions and space group determined photographically. The crystal was transferred to a Stoe-Siemens four-circle diffractometer, and accurate cell dimensions were determined from the centring of 20 strong reflections in the range $15 < 2\theta < 25°$. 3 993 Reflections were measured in the range $3.0 < 2\theta < 50.0°$ using graphite-monochromated Mo-K_α radiation and a 120-step ω/θ scan technique. The step width was fixed at 0.01° and the time for each step set at 0.5 s; backgrounds were measured for 15 s at each end of the scan. Reflections where the intensity was less than 4 counts s^{-1} in a 0.5 s prescan were not measured. Two check reflections were monitored periodically throughout data collection and showed no significant variation in intensity. A semi-empirical absorption correction based on a pseudo-ellipsoid model and 320 azimuthal scan data from 21 independent reflections was applied. Transmission factors ranged from 0.815 to 0.889 for the full data set. Lorentz polarisation corrections were applied and equivalent reflections averaged to give 1 398 unique observed reflections [$F > 5\sigma(F)$].

Structure Solution and Refinement.—For both (9) and (15) the metal atoms were located by multisolution Σ_2 sign expansion, and all the remaining non-hydrogen atoms from subsequent electron difference synthesis. The structure of (9) was refined by blocked full-matrix least squares with all the non-hydrogen atoms assigned anisotropic thermal parameters. The structure of (15) was refined by blocked-cascade least

squares with the Au, Ru, and P atoms assigned anisotropic thermal parameters, and the C and O atoms individual isotropic temperature factors. For both (9) and (15) the C–H atoms were placed in idealised positions (C–H 1.08 Å) and constrained to ride on the relevant C atom; in each case these H atoms were assigned a common isotropic temperature factor. In the final cycles of refinement of both (9) and (15) a weighting scheme of the form $w = [\sigma^2(F)]^{-1}$ was introduced.

For (9), the final R and R' were 0.034 and 0.035, and for (15), 0.067 and 0.056, where $R' = \Sigma w^{\frac{1}{2}}\Delta/\Sigma w^{\frac{1}{2}}|F_o|$. A final electron-density difference map for (15) showed ripples of *ca.* 1.5 e Å^{-3} close to the position of the Au atom but no other regions of significant electron density.

Complex neutral-atom scattering factors [30] were employed throughout both structure solution and refinements. Computations for both structures were performed using programs written by Professor G. M. Sheldrick.[31] The molecular plots were drawn using ORTEP 2.[32]

The final atomic co-ordinates are given in Tables 8 and 9 for compounds (9) and (15) respectively; bond lengths and angles are in Tables 4—7.

Acknowledgements

We thank the S.E.R.C. and Johnson Matthey for financial support and Dr. D. T. Thompson (Johnson Matthey) for valuable discussion.

References

1 F. Iwasaki, M. J. Mays, P. R. Raithby, P. L. Taylor, and P. J. Wheatley, *J. Organomet. Chem.*, 1981, **213**, 181.
2 K. Natarajan, O. Scheidsteger, and G. Huttner, *J. Organomet. Chem.*, 1981, **221**, 301.
3 J. S. Field, R. J. Haines, and D. N. Smit, *J. Organomet. Chem.*, 1982, **224**, C49.
4 S. A. Maclaughlin, A. J. Carty, and N. J. Taylor, *Can. J. Chem.*, 1982, **60**, 87.
5 G. Huttner, J. Schneider, H. D. Muller, G. Mohr, J. von Seyerl, and L. Wolfhart, *Angew. Chem., Int. Ed. Engl.*, 1979, **18**, 76.
6 C. U. Pittman, G. M. Wileman, W. D. Wilson, and R. C. Ryan, *Angew. Chem., Int. Ed. Engl.*, 1980, **19**, 478.
7 W. F. Smith, N. J. Taylor, and N. J. Carty, *J. Chem. Soc., Chem. Commun.*, 1976, 896.
8 A. J. Carty, *Adv. Chem. Ser.*, 1982, **196**, 163.
9 J. C. Bricker, C. C. Nagel, and S. G. Shore, *J. Am. Chem. Soc.*, 1982, **104**, 1444.
10 P. C. Ford, *Acc. Chem. Res.*, 1981, **14**, 31.
11 B. D. Dombek, *J. Am. Chem. Soc.*, 1981, **103**, 6508.
12 M. J. Mays, P. R. Raithby, P. L. Taylor, and K. Henrick, *J. Organomet. Chem.*, 1982, **224**, C45.
13 J. Schneider, L. Zsolnai, and G. Huttner, *Chem. Ber.*, 1982, **115**, 989.
14 J. Knight and M. J. Mays, *J. Chem. Soc., Dalton Trans.*, 1972, 1022.
15 J. Agapiou, S. E. Pedersen, L. A. Zyzyck, and J. R. Norton, *J. Chem. Soc., Chem. Commun.*, 1977, 393.
16 K. Henrick, M. J. Mays, and P. L. Taylor, *Acta Crystallogr., Sect. B*, 1982, **38**, 2261.
17 J. M. Fernandez, B. F. G. Johnson, J. Lewis, and P. R. Raithby, *Acta Crystallogr., Sect. B*, 1979, **35**, 1711.
18 H. Vahrenkamp and E. J. Wuchener, *Angew. Chem., Int. Ed. Engl.*, 1981, **20**, 680.
19 D. G. Evans and D. M. P. Mingos, *J. Organomet. Chem.*, 1982, **232**, 171.
20 B. F. G. Johnson, D. A. Kaner, J. Lewis, and P. R. Raithby, *J. Organomet. Chem.*, 1981, **215**, C33; B. F. G. Johnson, D. A. Kaner, J. Lewis, P. R. Raithby, and M. J. Taylor, *J. Chem. Soc., Chem. Commun.*, 1982, 314; K. Burgess, B. F. G. Johnson, D. A. Kaner, J. Lewis, P. R. Raithby, and S. N. A. B. Syed-Mustaffa, *J. Chem. Soc., Chem. Commun.*, 1983, 455.
21 M. Green, K. A. Mead, R. M. Mills, I. D. Salter, F. G. A. Stone, and P. Woodward, *J. Chem. Soc., Chem. Commun.*, 1982, 51.
22 L. W. Bateman, M. Green, J. A. K. Howard, K. A. Mead, R. M. Mills, I. D. Salter, F. G. A. Stone, and P. Woodward, *J. Chem. Soc., Chem. Commun.*, 1982, 773.
23 D. A. Edwards and J. Marshalsea, *J. Organomet. Chem.*, 1971, **131**, 73.
24 R. A. Schrock and J. A. Osborn, *J. Am. Chem. Soc.*, 1971, **93**, 2397.
25 L. M. Haines and E. Singleton, *J. Chem. Soc., Dalton Trans.*, 1972, 1891.
26 F. G. Mann, D. Purdie, and A. F. Wells, *J. Chem. Soc.*, 1936, 1503.
27 F. G. Mann, D. Purdie, and A. F. Wells, *J. Chem. Soc.*, 1937, 1828.
28 P. G. Jones, A. G. Maddock, M. J. Mays, M. M. Muir, and A. F. Williams, *J. Chem. Soc., Dalton Trans.*, 1977, 1434.
29 K. R. Adam, G. Anderegg, L. F. Lindoy, H. C. Lip, M. McPartlin, J. H. Rea, R. J. Smith, and P. A. Tasker, *Inorg. Chem.*, 1980, **19**, 2956.
30 'International Tables for *X*-Ray Crystallography,' Kynoch Press, Birmingham, 1974, vol. 4.
31 G. M. Sheldrick, 'SHELX 76,' Molecular Structure Determination Program Package, University of Cambridge, 1976.
32 C. K. Johnson, ORTEP 2, Oak Ridge National Laboratory, Tennessee.

Received 14*th July* 1983; *Paper* 3/1216